

Quantum oscillations in antiferromagnetic CaFe_2As_2 on the brink of superconductivity

This article has been downloaded from IOPscience. Please scroll down to see the full text article.

2009 J. Phys.: Condens. Matter 21 322202

(<http://iopscience.iop.org/0953-8984/21/32/322202>)

View [the table of contents for this issue](#), or go to the [journal homepage](#) for more

Download details:

IP Address: 129.252.86.83

The article was downloaded on 29/05/2010 at 20:42

Please note that [terms and conditions apply](#).

FAST TRACK COMMUNICATION

Quantum oscillations in antiferromagnetic CaFe_2As_2 on the brink of superconductivity

N Harrison, R D McDonald, C H Mielke, E D Bauer, F Ronning and J D Thompson

Los Alamos National Laboratory, MS-E536, Los Alamos, NM 87545, USA

Received 8 June 2009, in final form 2 July 2009

Published 20 July 2009

Online at stacks.iop.org/JPhysCM/21/322202

Abstract

We report quantum oscillation measurements on CaFe_2As_2 under strong magnetic fields—recently reported to become superconducting under pressures of as little as a kilobar. The largest observed carrier pocket occupies less than 0.05% of the paramagnetic Brillouin zone volume—consistent with Fermi surface reconstruction caused by antiferromagnetism. On comparing several alkaline earth AFe_2As_2 antiferromagnets (with $\text{A} = \text{Ca}, \text{Sr}$ and Ba), the dependences of the Fermi surface cross-sectional area F_α and the effective mass m_α^* of the primary observed pocket on the antiferromagnetic/structural transition temperature T_s are both found to be consistent with the case for quasiparticles in a conventional spin-density wave model. These findings suggest that the recently proposed strain-enhanced superconductivity in these materials occurs within a broadly conventional spin-density wave phase.

(Some figures in this article are in colour only in the electronic version)

The detection of magnetic quantum oscillations continues to be a powerful experimental method for determining the existence of Fermi surface reconstruction, often revealing the existence of small pockets of carriers [1–3] missed by other spectroscopic tools [4, 5]. In the recently discovered high T_c superconductors based on FeAs layers [6–11], they have played an essential role in establishing the existence of a Fermi surface within the parent antiferromagnetic state [3, 12]. As with cuprates and heavy fermion systems [13], the proximity of antiferromagnetism to superconductivity raises the prospect of antiferromagnetically-mediated superconductivity.

Among stoichiometric Sn flux-grown AFe_2As_2 antiferromagnets, CaFe_2As_2 lies closest in pressure phase space to superconductivity (see figure 1)—reported to exist at pressures as low as 1.4 kbar [14, 15], compared to ~ 30 kbar in its chemically closest relative SrFe_2As_2 [16]. Recent pressure experiments identify the superconductivity in CaFe_2As_2 to occur in a region of phase coexistence of orthorhombic/antiferromagnetic and collapsed tetragonal phases under non-ideal hydrostatic conditions [17], with strain playing an important (yet unspecified) role in its enhancement [18]. While neutron scattering experiments

reveal a clear segregation into orthorhombic and collapsed tetragonal domains [19], nuclear magnetic resonances studies indicate superconductivity to be associated with the orthorhombic volume fraction [20]. Tentative evidence for strain-enhanced superconductivity being generic to this family of antiferromagnets is found in stoichiometric non-Sn flux-grown samples of SrFe_2As_2 [21], where a partial superconducting volume fraction occurs without proximity to a collapsed tetragonal phase.

Given that superconductivity typically involves the pairing of quasiparticles within an otherwise metallic state, there exists considerable motivation for understanding the properties of the normal quasiparticles and their origin in AFe_2As_2 antiferromagnets. On comparing Sn flux-grown AFe_2As_2 crystals, both the required magnitude of the pressure p_s [14–16] and the order of the superconducting transition temperature T_c are sensitive to the interlayer lattice spacing c [22–24]. The sequential substitution of the alkali earth ion A with Ba, Sr , and Ca in figure 1 thus provides an analog to uniaxial pressure along the c -axis, giving rise to a possible evolution in the electronic properties that can be probed experimentally [25].

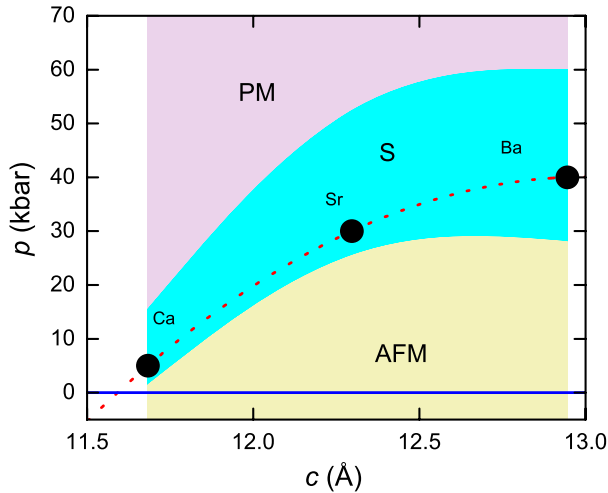


Figure 1. Schematic pressure p versus FeAs bilayer spacing c diagram for nominally stoichiometric Sn flux-grown $A\text{Fe}_2\text{As}_2$ single crystals, where $A = \text{Ca}, \text{Sr}$ and Ba , indicating the nominal regions where antiferromagnetism (AFM) and possible paramagnetic metallic behavior (PM) are reported. Superconductivity (S) may be associated with a region of phase coexistence or strain [15–17], suggesting that the precise conditions for its isolation remain to be identified. The black circles (and dotted line) represent the optimal pressure p_s with which superconductivity is reported to attain its highest value. The c values appropriate for the orthorhombic antiferromagnetic phase below T_s are taken from [22–24], while the p values are taken from [15, 16]. Lines are drawn between each of the compositions as guides for the eye.

In the present paper, we determine the Fermi surface of the most axially compressed member of this series, CaFe_2As_2 , by utilizing the contactless conductivity technique that has been successfully applied to SrFe_2As_2 [3] and BaFe_2As_2 [12], as well as the cuprate superconductors in strong magnetic fields [2, 26]. A sample of CaFe_2As_2 of dimensions $\approx 1 \times 1.5 \times 0.2 \text{ mm}^3$ is cut from a larger Sn flux-grown crystal [15] and mounted with its tetragonal c axis aligned parallel to the magnetic induction $\mathbf{B} \approx \mu_0\mathbf{H}$ (or rotated away from \mathbf{H} by an angle θ). Its planar face is attached to a 5 turn compensated coil of diameter $\approx 0.7 \text{ mm}$ that forms part of a tunnel diode oscillator (TDO) circuit. The TDO resonates at a frequency of $\approx 46 \text{ MHz}$ in the absence of an applied magnetic field, dropping by $\approx 200 \text{ kHz}$ in $\sim 60 \text{ T}$ in response to the magnetoresistivity of the sample. The associated increase in in-plane resistivity changes the coil inductance and resonance frequency, suggesting that the quantum oscillations (which reach a maximum amplitude at $\sim 60 \text{ T}$ of 1 part in a 1000 of the magnetoresistance) originate from the Shubnikov–de Haas (SdH) effect (with the observed effective masses being too heavy to be attributed to Sn inclusions). The TDO frequency is mixed down to $< 1 \text{ MHz}$ in two stages whereupon it is digitized at a rate of 20 MHz during the $\sim 50 \text{ ms}$ duration of the magnetic field pulse. The sample is immersed in gaseous or liquid ^3He throughout the experiments, with the temperature controlled through the vapor pressure for $T < 2 \text{ K}$ or by a heater for $T > 2 \text{ K}$ and measured using a calibrated cernox resistor (mounted close to the sample) immediately prior to the magnetic field pulse.

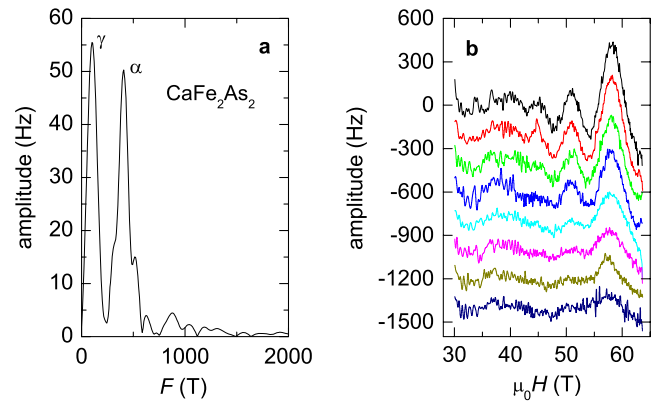


Figure 2. (a) Fourier transform of quantum oscillations in the TDO resonance frequency in $1/B$ at 0.98 K . (b) Raw TDO frequency oscillations for $\mathbf{H}||\mathbf{c}$ with curves at $T = 0.98, 1.52, 2.08, 3.1, 4.2, 5.0, 6.0$ and 7.0 K consecutively offset.

Figure 2 shows results of quantum oscillation experiments performed on CaFe_2As_2 , after subtracting a linear background and performing Fourier transformation in $1/B$. When $\mathbf{H}||\mathbf{c}$, several oscillations are discernible corresponding to a frequency $F_\alpha = 395 \pm 10 \text{ T}$, with another feature at $F_\gamma = 95 \pm 20 \text{ T}$ becoming more clearly discernible at higher T when the amplitude of F_α is thermally suppressed (here we use the frequency labeling scheme adopted for SrFe_2As_2 in [3]¹). A third frequency $F_\beta \sim 200 \text{ T}$, if present, is strongly reduced in amplitude compared to that in SrFe_2As_2 . On further performing a rotation study (presented in figure 3), both F_α and F_γ are found to be consistent with small ellipsoidal pockets in a similar fashion to SrFe_2As_2 [3], with the larger occupying less than 0.05% of the paramagnetic Brillouin zone volume. These findings support a scenario in which the Fermi surface is reconstructed as a consequence of the broken translational symmetry brought about by magnetic ordering, as was recently established in SrFe_2As_2 [3].

A significant finding in the current study is that the effective masses in CaFe_2As_2 exhibit only a small relative change compared to SrFe_2As_2 [3] or BaFe_2As_2 [12], in spite of CaFe_2As_2 being much more easily coerced towards superconductivity in figure 1. Figure 4 shows a fit of the Lifshitz–Kosevich theoretical [27] form $A = A_0X/\sinh X$ (where $X = 2\pi^2m_i k_B T/\hbar e B$) to the temperature-dependent quantum oscillation amplitude in CaFe_2As_2 . The fitted values of the effective mass are compared to those of similar pockets in SrFe_2As_2 and BaFe_2As_2 in table 1 and figure 5.

The absence of a divergence in the effective mass on reducing c in figure 5(a), or reducing the antiferromagnetic/structural transition temperature T_s in figure 5(b), is in marked contrast to recent observations made in heavy fermion antiferromagnets [28] and cuprate superconductors [29], where antiferromagnetic correlations strongly suppress the ability of the f - or d -electrons to participate in electrical conduction. Given that the Fermi velocities and/or effective masses in FeAs-layered systems are renormalized by only a factor a two

¹ Note that the α and β are mistakenly interchanged in figure 2(b) of [3] and in the discussion section of [3] relating the pockets to the bandstructure calculations.

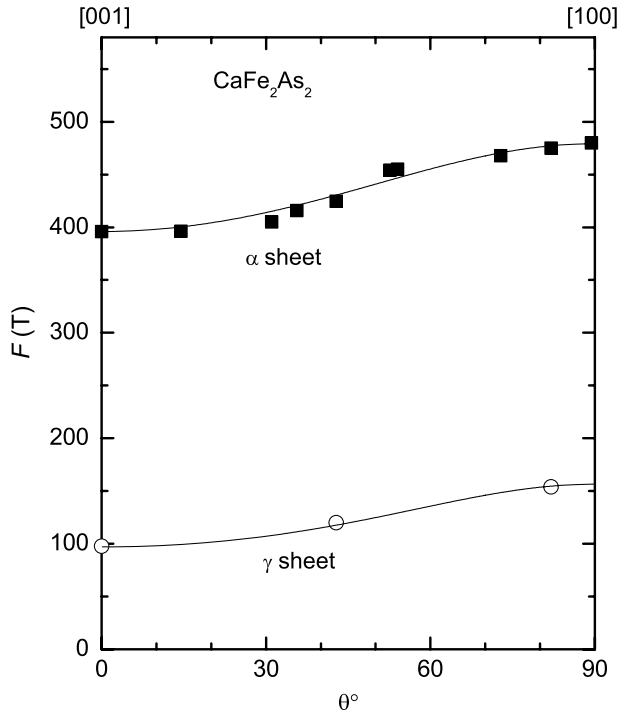


Figure 3. Magnetic field orientation-dependence of the α and γ quantum oscillation frequencies determined by Fourier transformation, where $\theta = 0$ corresponds to $\mathbf{H}\parallel\mathbf{c}$ and $\theta = 90^\circ$ corresponds to $\mathbf{H}\parallel\mathbf{a}$ at room temperature. The sample and coil are rotated *in situ*.

Table 1. Values of the Fermi surface frequencies F_i and effective masses m_i for $\mathbf{H}\parallel\mathbf{c}$, taken from this work and [3, 12]. Also shown, is the structural transition temperature T_s into the orthorhombic, antiferromagnetic phase.

A	T_s (K)	F_α (T)	m_α^* (m_e)	F_γ (T)	m_γ^* (m_e)
Ca	170	395	1.8 ± 0.2	95	1.0 ± 0.2
Sr	200	370	2.0 ± 0.1	70	—
Ba	138	430	1.2 ± 0.3	95	0.9 ± 0.1

compared to bandstructure estimates [3, 12], the physics of AFe_2As_2 appears to be much closer to that of a conventional spin-density wave [30], with the on-site Coulomb repulsion between the d-electrons being insufficiently strong to cause development of a Mott insulating state. In the case of a conventional spin-density wave, antiferromagnetic correlations lead to a comparatively weak enhancement of m^* that increases with the size of the spin-density wave gap 2Δ [31]. A suppression of T_s is not expected to lead to a divergence in m^* inside the antiferromagnetic phases in such a case.

Possible evidence for conventional spin-density wave ordering in AFe_2As_2 is provided in figure 5(b) by the reduction in the size of the pocket F_α and weak enhancement of m_α^* on increasing T_s (which varies non-monotonically with A and c). Here, we concentrate on the larger pocket that is observed consistently in all antiferromagnetic AFe_2As_2 compounds, which also contributes most to the electronic heat capacity on account of its larger surface area. The observed trends in figure 5(b) can be understood by considering a simplified spin-

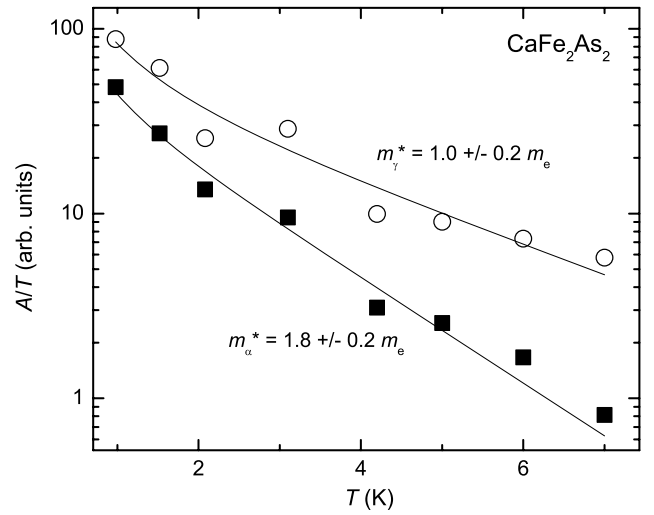


Figure 4. Temperature-dependence of A/T for $\mathbf{H}\parallel\mathbf{c}$ together with fits to the Lifshitz–Kosevich theory as described in the text. Fitted values of the effective mass are shown, where m_e is the free electron mass.

density wave reconstruction model (see figure 5(c)) in which the spin-density wave gap 2Δ increases with the transition temperature T_s . If the unreconstructed Fermi surfaces are assumed to be similar throughout [3], the progressive increase in 2Δ incurred on going from Ba to Ca to Sr improves the effectiveness of nesting, resulting in a progressive reduction in the sizes of the pockets and a gradual flattening of the reconstructed band leading to the enhancement in m^* .

The coupling of the spin or charge modulation to the lattice distortion at T_s affects the order of the transition, likely causing some degree of departure from the BCS relation, $\Delta = 1.76k_B T_s$ [32]². On the other hand, quantitative consistency with the spin-density wave model is found on comparing the reduction δE in the filling E of the pocket with the increase $\delta\Delta$ in Δ on going from A = Ca to Sr (which have the smallest percentage error bars in m_α^*). If we assume a parabolic dispersion whereby $E = \hbar e F_\alpha / m_\alpha^*$ and a BCS gap (as a first approximation), we arrive at quantitatively similar incremental changes $\delta E \approx 4 \pm 2$ meV and $\delta\Delta \approx 4.5$ meV (estimated using the BCS relation [32] (see footnote 2)) as expected for the simple spin-density wave model presented in figure 5(c).

Hence, while the experimental conditions required to optimize superconductivity in stoichiometric AFe_2As_2 compounds remain to be characterized, a comparison of the Fermi surface properties of CaFe_2As_2 with those of SrFe_2As_2 and BaFe_2As_2 reveals that the effective masses and pocket sizes exhibit a dependence on the antiferromagnetic/structural transition temperature T_s . Such a finding is consistent with weakly enhanced quasiparticles moving in an antiferromagnetic background of spins, suggesting that antiferromagnetism in AFe_2As_2 can be effectively understood from the perspective of a conventional spin-density wave.

² We are neglecting the effect of the coupling to the lattice, which likely causes the transition to become of first order near T_s . Coupling to the lattice typically increases the size of the gap compared to that obtained from the BCS estimate [32].

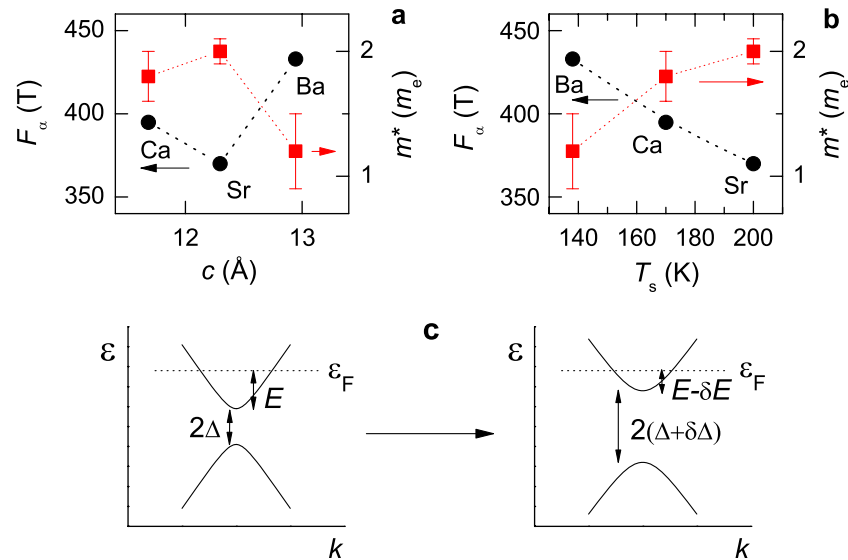


Figure 5. Plots of the largest quantum oscillation frequency F_α for $\mathbf{H}\parallel\mathbf{c}$ (left-hand axis) and effective mass m^* (right-hand-axis) versus the bilayer spacing (a) and the structural transition temperature T_s (b) from the high temperature tetragonal phase into the low temperature orthorhombic, antiferromagnetic phase. (c) A one-dimensional schematic showing how the size of the pocket ($\propto F$) is inversely related to the size of the spin-density wave gap ($2\Delta \propto T_s$). In the simplest model, an increase $\delta\Delta$ in Δ leads to an equal and opposite reduction δE in the filling E of the pocket (for a constant Fermi energy ϵ_F).

Given that superconductivity can occur within orthorhombic phase of AFe_2As_2 [18, 19], the existence of small pockets of carriers (now identified to be a universal feature of these compounds) are crucial prerequisite for its coexistence with antiferromagnetism, as recently found in CeIn_3 [36]. The present experiments reveal the magnitude of the superconducting transition temperature to be more closely correlated with the inter-layer spacing (i.e. [16] and figure 1) than it is with the degree of effective mass enhancement. Such a correlation between transition temperature and layer spacing is found in other families of layered superconductors [33–35]. The primary effect of the close proximity to the ‘collapsed tetragonal phase’ in CaFe_2As_2 therefore appears to be in instigating superconductivity by precipitating strain under non-ideal hydrostatic conditions. If the orthorhombic distortion is a necessary prerequisite for long range antiferromagnetism in this series of compounds, by suppressing the geometric frustration between neighboring Fe moments that would otherwise occur [37], then its vulnerability to an in-plane strain component could be an important factor in tuning superconductivity.

This work is conducted under the auspices the US Department of Energy, while the National High Magnetic Field Laboratory, where the experiments were conducted, is primarily funded by the National Science Foundation and the State of Florida.

References

- [1] Doiron-Leyraud N *et al* 2007 *Nature* **447** 565
- [2] Yelland E A *et al* 2008 *Phys. Rev. Lett.* **100** 047003
- [3] Sebastian S E *et al* 2008 *J. Phys.: Condens. Matter* **20** 422203
- [4] Hossain M A *et al* 2008 *Nat. Phys.* **4** 527
- [5] Liu H Y *et al* 2008 *Phys. Rev. B* **78** 184514
- [6] Kamihara Y *et al* 2008 *J. Am. Chem. Soc.* **130** 3296
- [7] Takahashi H *et al* 2008 *Nature* **453** 376
- [8] Chen X H *et al* 2008 *Nature* **453** 761
- [9] Ren Z-A *et al* 2008 *Europhys. Lett.* **82** 57002
- [10] Ren Z-A *et al* 2008 *Mater. Res. Innov.* **12** 106
- [11] Liu R H *et al* 2008 *Phys. Rev. Lett.* **101** 087001
- [12] Mazin I I *et al* 2008 *Phys. Rev. Lett.* **101** 057003
- [13] Analytis J G *et al* 2009 arXiv:0902.1172
- [14] Monthoux P, Pines D and Lonzarich G G 2007 *Nature* **450** 1177
- [15] Torikachvili M S *et al* 2008 *Phys. Rev. Lett.* **101** 057006
- [16] Park T *et al* 2008 *J. Phys.: Condens. Matter* **20** 322204
- [17] Lee H *et al* 2008 arXiv:0809.3550
- [18] Alireza P *et al* 2009 *J. Phys.: Condens. Matter* **21** 012208
- [19] Yu W *et al* 2009 *Phys. Rev. B* **79** 020511
- [20] Canfield P C *et al* 2009 arXiv:0901.4672
- [21] Canfield P C *et al* 2009 *Physica B* at press
- [22] Goldman A L *et al* 2009 *Phys. Rev. B* **79** 024513
- [23] Baek S-H *et al* 2009 arXiv:0903.2011
- [24] Saha S R *et al* 2008 arXiv:0811.3940
- [25] Kreyssig A *et al* 2008 *Phys. Rev. B* **78** 184517
- [26] Tegel M *et al* 2008 *J. Phys.: Condens. Matter* **20** 452201
- [27] Rotter M *et al* 2008 *Phys. Rev. B* **78** 020503
- [28] Tompsett D A and Lozarich G G 2009 arXiv:0902.4859
- [29] Sebastian S E *et al* 2008 *Nature* **454** 200
- [30] Shoenberg D 1984 *Magnetic Oscillations in Metals* (Cambridge: Cambridge University Press)
- [31] Shishido H *et al* 2005 *J. Phys. Soc. Japan* **74** 1103
- [32] Sebastian S E *et al* 2008 *Workshop on Cuprate Fermiology (Maryland)*
- [33] Hertz J A 1976 *Phys. Rev. B* **14** 1165
- [34] Millis A J 1993 *Phys. Rev. B* **48** 7183
- [35] McDonald R D *et al* 2005 *Phys. Rev. Lett.* **94** 106404
- [36] Grüner G 1994 *Density Waves in Solids, Frontiers in Physics* vol 89 (Reading, MA: Addison-Wesley)
- [37] Rotter M, Tegel M and Johrendt D 2008 *Phys. Rev. Lett.* **101** 107006
- [38] Sasmal K *et al* 2008 *Phys. Rev. Lett.* **101** 107007
- [39] Schrieffer J R and Brooks J S (ed) 2007 *High-Temperature Superconductivity Theory and Experiment* (Berlin: Springer)
- [40] Bauer E D *et al* 2004 *Phys. Rev. Lett.* **93** 147005
- [41] Sebastian S E *et al* 2009 *Proc. Natl Acad. Sci. USA* **106** 7741
- [42] Si Q and Abrahams E 2008 arXiv:0804.2480